

Transactions, SMiRT-26
Berlin/Potsdam, Germany, July 10-15, 2022
Division V

PARAMETRIC STUDY OF CONTACT CONDITIONS FOR SC WALLS SUBJECT TO OUT-OF-PLANE DYNAMIC LOADING

Eric Kjolsing¹, Mark Weaver², and Joseph Magallanes³

¹ Senior Engineer, Karagozian & Case, Glendale, CA, USA (kjolsing@kcse.com)

² Principal, Karagozian & Case, Glendale, CA, USA

³ President, Karagozian & Case, Glendale, CA, USA

ABSTRACT

Most of the out-of-plane experimental studies of steel plate composite (SC) walls have used tie bars instead of tie plates. It has been postulated that tie plates with high aspect ratios (i.e., tie plates with wide widths) may lower the out-of-plane shear capacity of the SC wall as concrete interlock is eliminated along the slip planes between the tie plates and concrete infill. This paper presents a parametric study of contact conditions for an SC wall section subject to out-of-plane dynamic loading. The study is performed in LS-DYNA and uses a generalized cross section comprised of wall and plate sizes typical for nuclear construction. Tie plates, spanning between the exterior face plates, are modeled with two height-to-width aspect ratios. The interaction between the SC wall steel plates and concrete infill is established through contact definitions. The contact definitions are varied and include frictionless contact, several contacts with varying friction coefficients, and tied contact (i.e., fully bonded). The system is subjected to both impact and blast loading (i.e., high-energy, low duration) out-of-plane loading. The performance of the various configurations is compared. The results indicate that the load carrying capacity of the system depends on the tie plate aspect ratio and the friction modeled.

INTRODUCTION

Steel plate composite (SC) walls are seeing increased consideration in the design of new nuclear facilities. This is possible, in part, due to an extensive research effort to characterize the performance of these structural elements (note the work out of Purdue University) and develop design guidance such as AISC (2017). Recent conceptual designs for SC walls have utilized steel tie plates, instead of tie bars, to tie the exterior faceplates together. It has been postulated that tie plates with high aspect ratios (i.e., tie plates with wide widths) may lower the out-of-plane shear capacity of the SC wall as concrete interlock is eliminated along the slip planes between the tie plates and concrete infill.

An analytical study is performed in LS-DYNA (Release 12) to determine how, and to what degree, the out-of-plane load carrying capacity of an SC wall section changes as the aspect ratio of the tie plates is changed. Two aspect ratios are considered: 6:1 and 24:1. In both cases the cross-sectional area of the tie plates is held constant. Since load may be transferred between the concrete infill and steel tie plates through friction, the study also varies the friction coefficient within the models. The models are subjected to transient out-of-plane loading representative of high-energy, low duration events.

ANALYSIS MODEL

Model Geometry

The model geometry is shown in Figure 1. The steel faceplates are modeled as 0.875in thick (Case A) or 1.5in thick (Cases B, C, and D); thicker faceplates are used in models B, C, and D to increase the flexural capacity of the wall and promote a shear failure, which is the failure mechanism of interest in this study. Shear studs are modeled with a 6in embedment and are spaced 8in x 4in. The stud diameter is 0.75in (Case A) or 1in (Cases B, C, and D). The stud diameter and spacing is selected to minimize stud failure, thus maximizing composite action and flexural capacity of the section. The steel tie plates are modeled as 6in x 1in (Cases A, B, and D) or 12in x 0.5in (Case C) and spaced at 16in; note that the tie plate area is 6in² in all cases. The SC wall section has a clear span of 144in resulting in a span-to-depth ratio of ~3:1; the span is intentionally small to promote a shear failure which is the mechanism of interest in this study. The SC wall section is supported by two support blocks, each 48in x 48in. The geometric parameters varied between each case are summarized in Table 1.

The +Y face of the supporting blocks are fixed to provide out-of-plane restraint to the model. Since the modeled SC wall section is intended to represent a portion of a larger wall, the +Z and -Z faces of the SC wall section and support blocks are restrained in the Z-direction.

Each shear stud is analytically merged to the concrete infill to ‘embed’ the stud. The head of each shear stud is merged to the adjacent steel faceplate to facilitate composite action. The ends of each tie plate are also merged to the adjacent faceplate. In most models, interaction between the faceplate-to-concrete infill and tie plate-to-concrete infill is defined with a contact definition utilizing different friction coefficients (*CONTACT_AUTOMATIC_SURFACE_TO_SURFACE). The exception to this is the ‘Tied’ models, where the faceplates and tie plates are completely merged to the concrete infill. Frictionless contact is defined between the SC wall section and support blocks for all models.

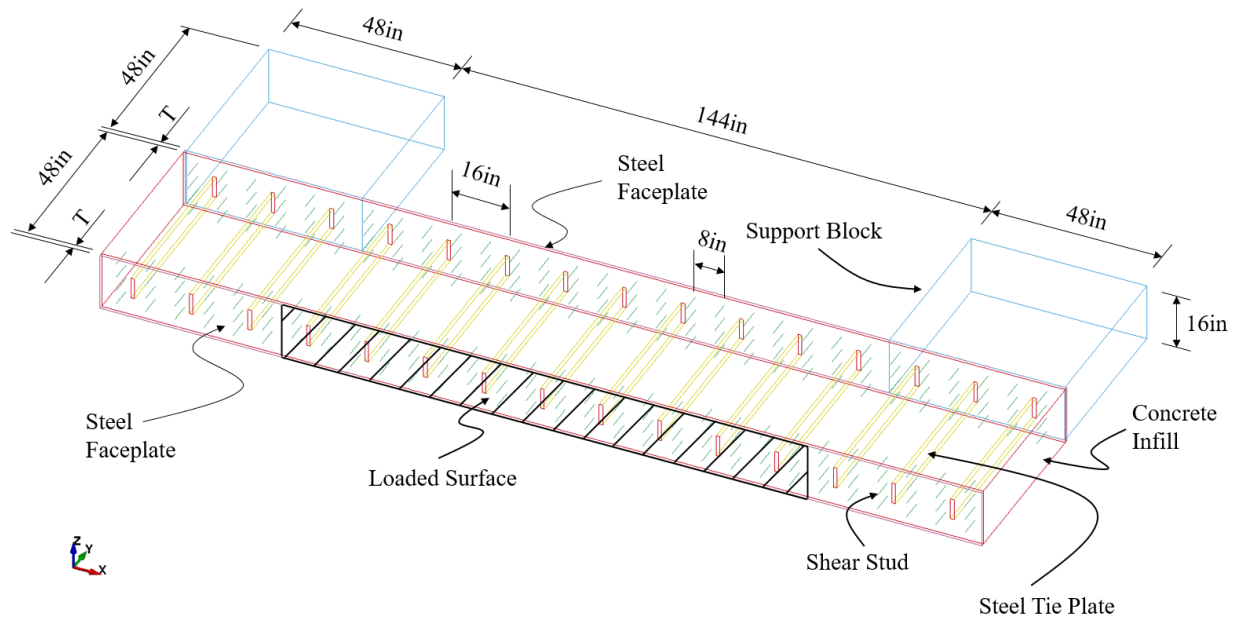


Figure 1. Model geometry (Case A shown).

Material Properties

The steel faceplates and tie plates are modeled as ASTM A572 Grade 50 steel. The expected dynamic material strength includes strain rate dependency. Deletion criteria of 5% maximum principal strain and 7% effective strain are included based on guidance from NEI (2011). The steel is modeled with the

LSDYNA material card 24 (*MAT_PIECEWISE_LINEAR_PLASTICITY) and thick shell elements (ELFORM=1) with hourglass control (IHQ=3). For convenience, the shear studs are modeled with the same material model, and beam elements (ELFORM=1).

The concrete infill is modeled with solid elements (ELFORM=1) with hourglass control (IHQ=3). The infill is modeled as 5ksi concrete, increased to 8ksi to account for a static increase factor and aging factor per NEI (2011); note that a dynamic increase factor is not included in the strength definition as the material model used in this study includes strain rate effects directly. The infill is modeled with the Karagozian & Case concrete constitutive model that is included in LSDYNA as material card 72R3 (*MAT_CONCRETE_DAMAGE_REL3). As described in Magallanes et al. (2016) this model:

- Utilizes three-invariant strength surfaces to account for pressure-dependence and differences in triaxial extension and compression.
- Includes the effects of shear-dilatancy and confinement, capturing increased compressive strength and ductility when appropriate.
- Captures material hardening and softening.
- Includes material strength enhancement at high strain rates.

The support blocks are modeled as elastic with properties corresponding to 8ksi concrete. An elastic material is selected so that the supports will not dissipate energy (through damage), allowing a more direct comparison of load carrying capacity of the SC wall configurations across the various realizations assessed.

Loading

Two different transient loads are considered: an ‘Airplane’ load and a ‘Blast’ load. The airplane load linearly ramps up a uniform pressure over the loaded surface (see Figure 1), holds the applied pressure (P_{applied}) constant for a finite duration, then ramps the load back down to zero. The duration of loading is significantly longer than the natural period of the system (T_n). The blast load applies a triangular pressure pulse on the loaded surface, with the maximum applied pressure occurring at time zero, then ramping back down to zero pressure over a duration that coincides with the natural period of the system. The natural period of the system is obtained from a free-vibration analysis of the ‘Tied’ Case D model. The airplane load is applied to Cases A, B, and C while the blast load is applied to Case D.

To obtain the load carrying capacity of the system, incrementally increasing load curves are applied to the model, and the behavior of the SC wall recorded. So, noting Figure 2, load curve i associated with $P_{\text{applied},i}$ is applied to an undamaged SC wall section, and the behavior of the wall recorded. Then load curve $i + 1$ associated with $P_{\text{applied},i+1}$ is applied to an undamaged SC wall section, and the behavior of the wall recorded. This process is repeated numerous (n) times to ensure that the failure mechanism and associated pressure is properly identified for each Case (A-D).

Note that while the airplane and blast load curves used in this study are not safeguarded information, they are intentionally obscured as a precautionary measure. Similarly, the load carrying capacities obtained from these analyses are normalized in the results section.

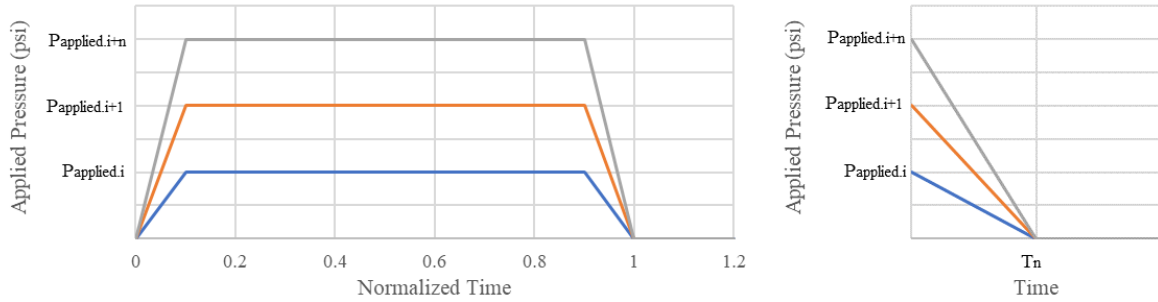


Figure 2. Methodology to determine load carrying capacity. ‘Airplane’ (left) and ‘Blast’ load (right).

Varied Parameters

As discussed above, four cases are modeled, as shown in Table 1. For each of the four cases, the following friction coefficients are assessed: $\mu = \mu_{\text{static}} = \mu_{\text{dynamic}} = 0.00, 0.02, 0.10, 0.50, 1.00$. Recall that these friction coefficients are applied to the contact definition between the steel plates and concrete infill. In addition, a model that ties the steel plates to the concrete infill is also assessed. This results in six contact variations of four models, or twenty-four model realizations, each subjected to an array of incrementally increasing load curves. In total, 329 realizations are assessed as part of this study.

Table 1. Case details.

Case	A	B	C	D
Faceplate Thickness, T	0.875in	1.5in	1.5in	1.5in
Shear Stud Diameter	0.75in	1in	1in	1in
Tie Plate Geometry	6in x 1in	6in x 1in	12in x 0.5in	6in x 1in
Loading	‘Airplane’	‘Airplane’	‘Airplane’	‘Blast’

RESULTS AND DISCUSSION

Table 2 presents normalized applied pressures associated with different failure mechanisms (P_{nf}) for each model realization. The values are normalized to the applied pressure associated with failure for Case B, $\mu=0.50$, as shown in Equation 1. Next to each numeric result is an indication of the associated failure mechanism: (F) = flexure, (S) = shear. The results are discussed for each of the four cases in the following sub-sections.

Table 2. Normalized applied pressure associated with failure, P_{nf} .
 Pressure normalized to Case B, $\mu=0.50$.

Friction Coefficient, μ	Case	A	B	C	D
	0.00	59% (F)	88% (S)	65% (S)	88% (F) - ... - 152% (S)
0.02	58% (F)	91% (S)	72% (S)	89% (F) - ... - 140% (S)	
0.10	58% (F)	99% (S)	80% (S)	97% (F) - ... - 141% (S)	
0.50	57% (F)	100% (F)	92% (S)	97% (F) - ... - 180% (S)	
1.00	57% (F)	100% (F)	97% (S)	96% (F) - ... - 183% (S)	
Tied	56% (F)	96% (F)	105% (F)	89% (F) - ... - 316% (S)	

$$P_{nf} = \frac{P_{\text{applied@failure}}}{P_{\text{applied@failure[Case B,}\mu=0.50]}} \quad (1)$$

Case A

All six model realizations for Case A display a flexural failure, which is likely why the load carrying capacity appears insensitive to the modeled friction coefficient ($P_{nf} = 56\%-59\%$ per Table 2). Representative analysis results are shown in Figure 3 and Figure 4. Figure 3 presents the shear strain in the concrete infill, just prior to failure, for the $\mu = 0.00$ and $\mu = 0.50$ model realizations. While both model realizations present characteristic flexural and shear cracks, the $\mu = 0.00$ result includes a vertical shear crack across the reduced section at shear ties 4 and 12. Since the capacity of Case A is governed by flexure, the influence of this shear crack on the load carrying capacity appears negligible. Figure 4 presents the plastic strain in the steel faceplates and tie plates, just prior to failure, for the $\mu = 0.00$ model realization (other Case A model realizations present similar results). Plastic strain is seen across the tension faceplate while high plastic strains are observed at the tie plate-to-faceplate connection. The flexural failure initiates in the faceplate (next to the tie plate) and then ‘unzips’ across the tension faceplate width as the deletion criteria removes the over-strained faceplate elements. The concentrated plastic strain at the tie plate-to-faceplate interface is discussed in detail in the following sub-sections.

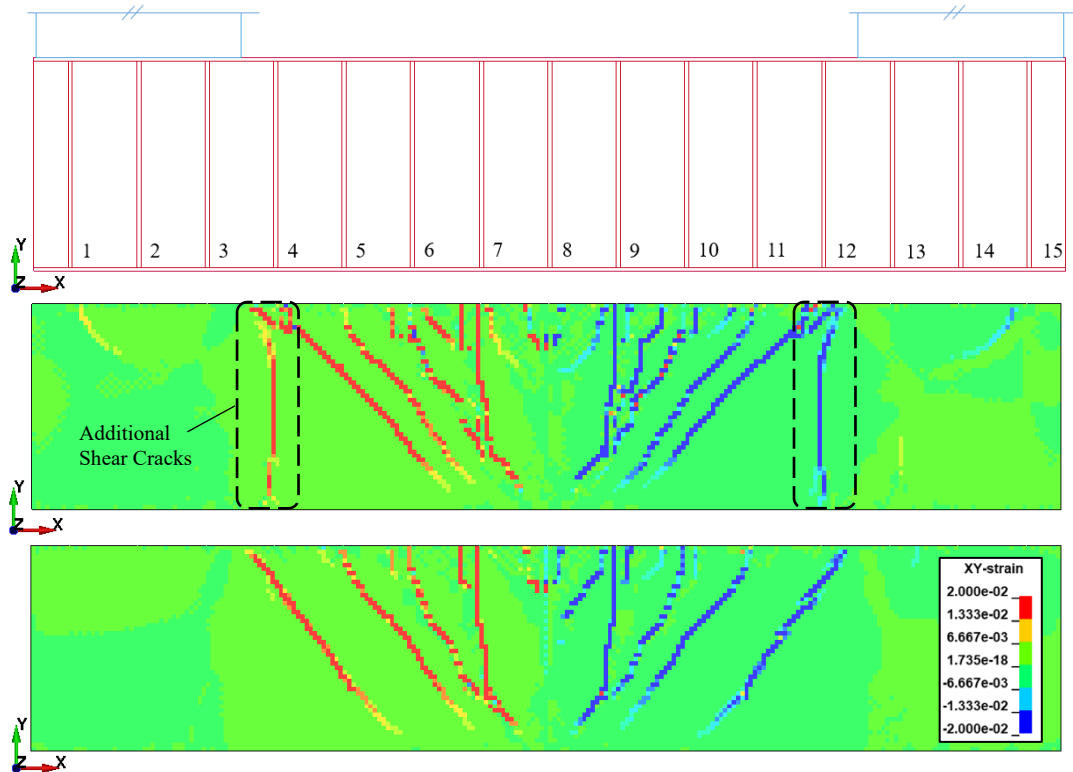


Figure 3. Case A concrete infill shear strain just prior to failure. Outline (top); ϵ_{xy} for $\mu = 0.00$, $P_{n,\text{applied}} = 59\%$ (middle) and $\mu = 0.50$, $P_{n,\text{applied}} = 57\%$ (bottom). Legend = $\pm 2\%$. Displacement scale = 0.

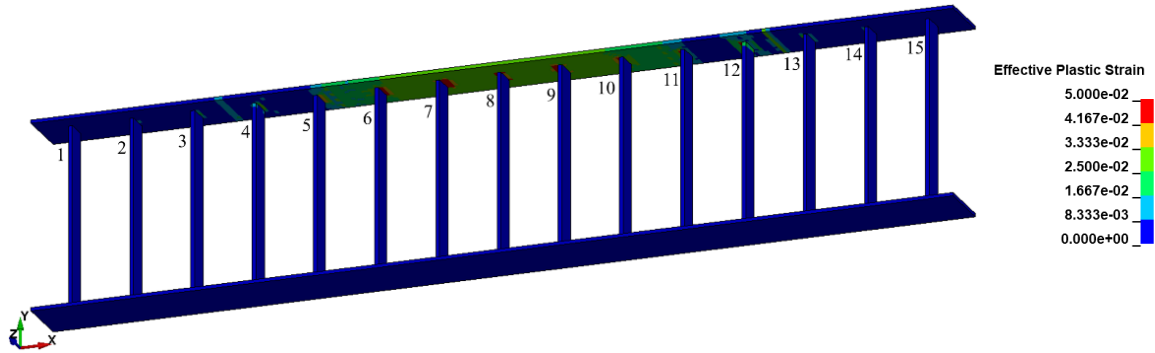


Figure 4. Case A steel plate effective plastic strain just prior to failure.
 $\mu = 0.00$, $P_{n,applied} = 59\%$. Legend = 0-5%. Displacement scale = 0.

Case B

Relative to Case A, the faceplate thickness in Case B is 71% larger (i.e., 1.5in / 0.875in = 171%). Since Case A is governed by a flexural failure, the expected Case B P_{nf} for flexure is $[56-59\%] \times 1.71 = [96-101\%]$, which is indeed observed in the three realizations demonstrating a flexural failure. A smaller normalized pressure is seen in the $\mu = 0.00$ and $\mu = 0.02$ model realizations, where a shear failure is seen to occur around $P_{nf} = 90\%$. Figure 5 shows representative analysis results from the $\mu = 0.00$ model realization where the same vertical shear crack along tie plates 4 and 12 are seen (recall Figure 3), but the extent and magnitude of significant shear strain is increased. By amplifying the displacement scale in LS-DYNA, a large, concentrated shear displacement is seen between the support block and tie plates 4 and 12. A review of the analysis results implies the following failure sequence: (a) the concrete infill across the reduced section at shear ties 4 and 12 undergoes large shear strain and a loss of shear strength/stiffness, (b) the reduced stiffness and low friction coefficient cause a large shear displacement between the supports and the adjacent tie plates, (c) the large, localized displacement imposes a rotation demand on the connection between the faceplate and tie plates 4 and 12 (which are restrained by the concrete infill and unable to rotate to alleviate the demand), (d) the combined axial strain in the tie plate (due to the remaining shear load being supported) and the additional strain on the tie plate (due to the localized rotation demand adjacent to the faceplate) exceed the strain criteria and the tie plate connection to the faceplate is lost, (e) having lost both the tie plates (4 and 12) and the adjacent concrete infill all shear capacity is lost and failure has occurred. This sequence is also observed in Case C, as discussed in the next sub-section.

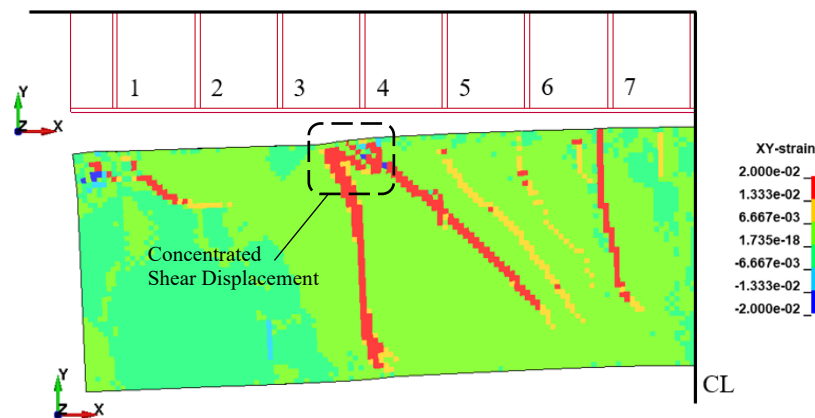


Figure 5. Case B concrete infill shear strain just prior to failure.
 Outline (top); ϵ_{xy} for $\mu = 0.00$, $P_{n,applied} = 88\%$ (bottom). Legend = +/-2%. Displacement scale = 3.

Case C

The Case C results indicate the same failure sequence as described in the Case B sub-section above. Case C is seen to have a lower load carrying capacity when compared to Case B for each friction considered (a decrease of up to 26% for the frictionless realization) and each of the friction model realizations now displays a shear failure mechanism. For a typical concrete-to-steel friction value (e.g., $\mu = 0.50$) the reduction in load carrying capacity, based on the assessed aspect ratios, is $\sim 8\%$. This indicates that the load carrying capacity of the section depends on the aspect ratio of the steel tie plates with large aspect ratio (i.e., wide) tie plates corresponding to a reduced load carrying capacity.

Figure 6 and Figure 7 show the concrete infill shear strain and steel plate plastic strain, respectively, for the same level of loading ($P_{n,applied} = 71\%$), across the contact conditions considered. At this load the $\mu = 0.00$ model realization has failed in shear (see Table 2) and a significant amount of shear strain is visible in Figure 6. The $\mu = 0.02$ model realization is on the verge of failure, but significantly less shear strain is visible. This is attributed to the brittle nature of a shear failure – catastrophic cracking is not apparent until failure has occurred. The ‘Tied’ model realization fails to predict the localized concrete cracking (adjacent to the tie plates) at this load level (compare the strain patterns of the ‘Tied’ model realization to those associated with the $\mu = 0.50$ and 1.00 model realizations). Other ‘Tied’ results (i.e., $P_{n,applied}$ just slightly less than P_{nf}) do indicate some concrete degradation adjacent to tie plates 4 and 12, but the extent of cracking is minimal; the ‘Tied’ model realization does not capture the shear failure mechanism predicted by the other Case C model realizations.

The $\mu = 0.00$ model realization in Figure 7 shows failure of the tie plate elements connecting the tie plate to the faceplate, as well as (subsequent) failure of the tension faceplate next to the support block. Higher levels of friction show reduced plastic strain in the steel plates at this level of loading.

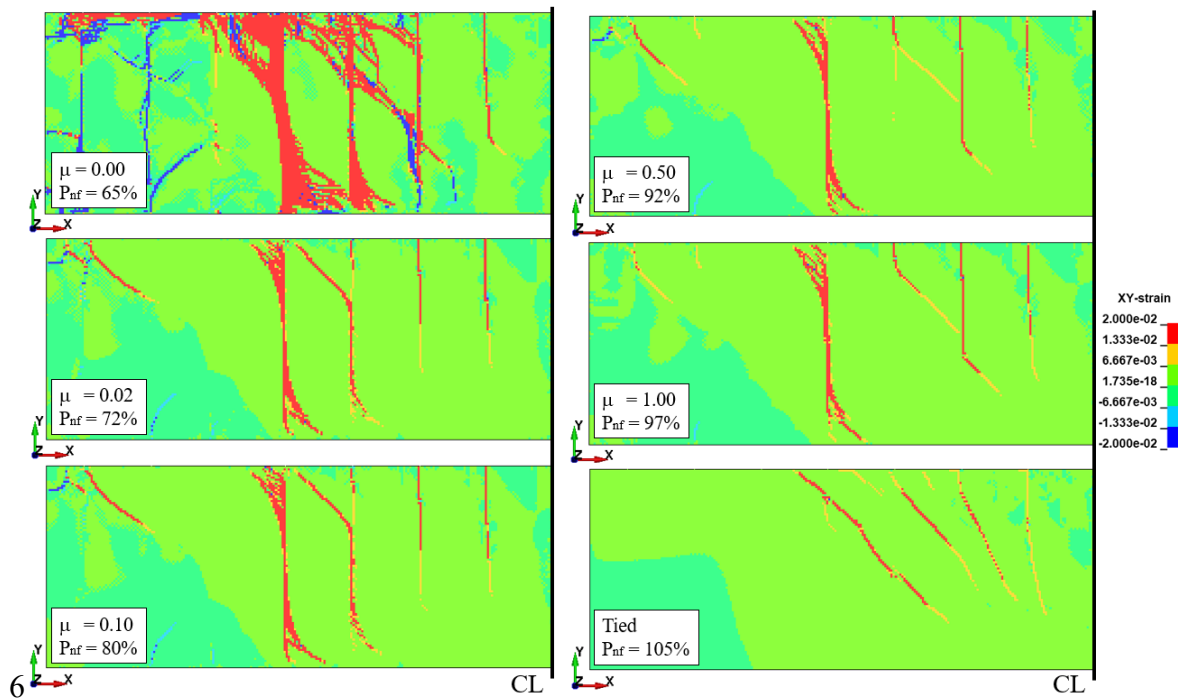


Figure 6. Case C concrete infill shear strain.
 $P_{n,applied} = 71\%$. Legend = $\pm 2\%$. Displacement scale = 0.

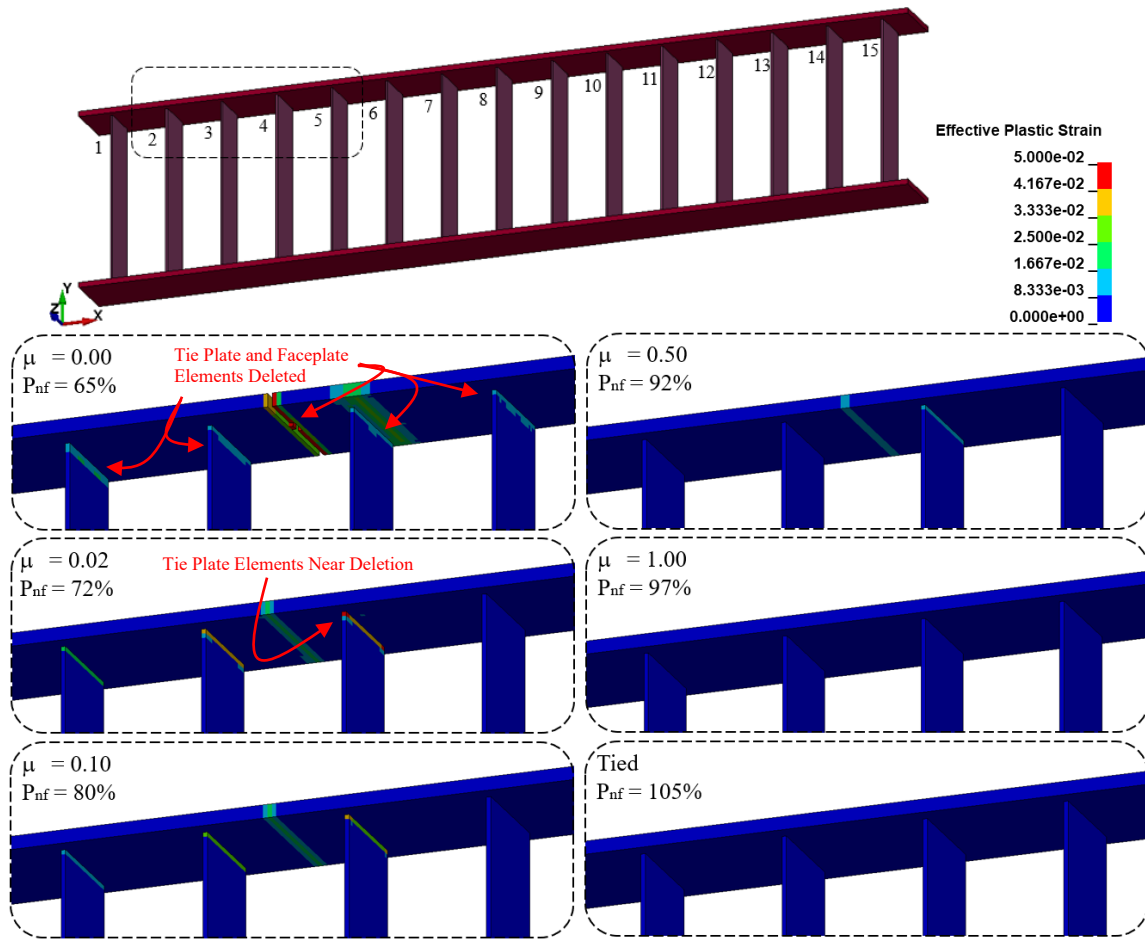


Figure 7. Case C steel plate effective plastic strain.
 $P_{n,applied} = 71\%$. Legend = 0-5%. Displacement scale = 0.

Case D

The Case D results cannot be directly compared to Cases A, B or C as the load curve is significantly different (see Figure 2). An initial flexural failure (deletion of tension faceplate elements) is observed for all Case D model realizations with P_{nf} ranging from 88%-97% per Table 2. With increasing overpressure (i.e., $P_{n,applied} > \text{Flexural } P_{nf}$) the failure mechanism is seen to evolve from a flexural failure to a shear failure. This evolving failure mechanism is due to an early phase rigid body shear response, followed by a subsequent (time delayed) flexural response; if the system can survive the early shear demand, it may still succumb to the subsequent flexural demand. The second set of P_{nf} values provided in Table 2 lists the pressures associated with the first observed instance of a pure shear failure for each model realization. Figure 8 shows the various failure mechanisms for the $\mu = 0.50$ model realization with incrementally increasing load curves. The system is seen to survive the loading in the first plot, a flexural failure is observed in the second plot, the failure is transitioning from a flexural failure to a shear failure in the third plot, and a shear failure is shown in the fourth plot. The results still imply a dependency on friction, but additional investigation is required to formalize the relationship.

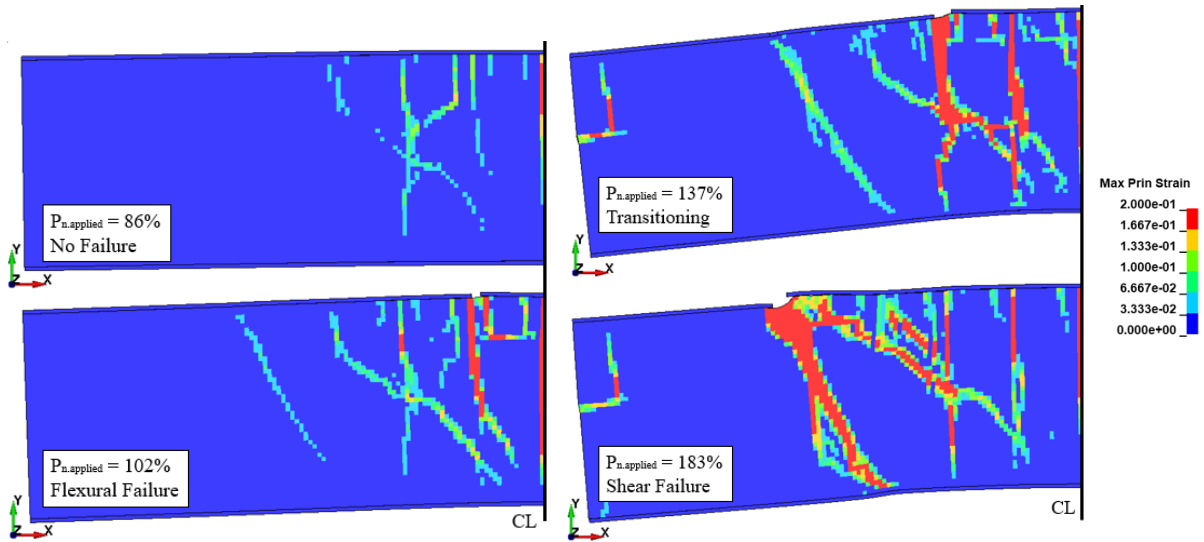


Figure 8. Case D concrete infill maximum principal strain; exterior steel faceplates are visible. $\mu = 0.50$. Legend = 0-20%. Displacement scale = 1.

Tied Model Realizations

The ‘Tied’ model realizations consistently predict a flexural failure. Originally noted in the Case C discussion (see Figure 6), the ‘Tied’ model realizations do not predict significant shear strain at the tie plate 4 and 12 locations. Figure 9 repeats this finding as only Case C shows a slight shear crack next to tie plate 4. When the concrete is tied to the tie plates, the plates appear to resist the xy shear strain at the tie plate location, preventing significant shear displacement near the support (and the subsequent failure/deletion of the tie plate connection to the faceplate), in turn preventing the shear failure seen in the other friction-based model realizations. The tied condition seems to artificially remove (or better put, unconservatively increase the capacity of) a potential shear failure mechanism.

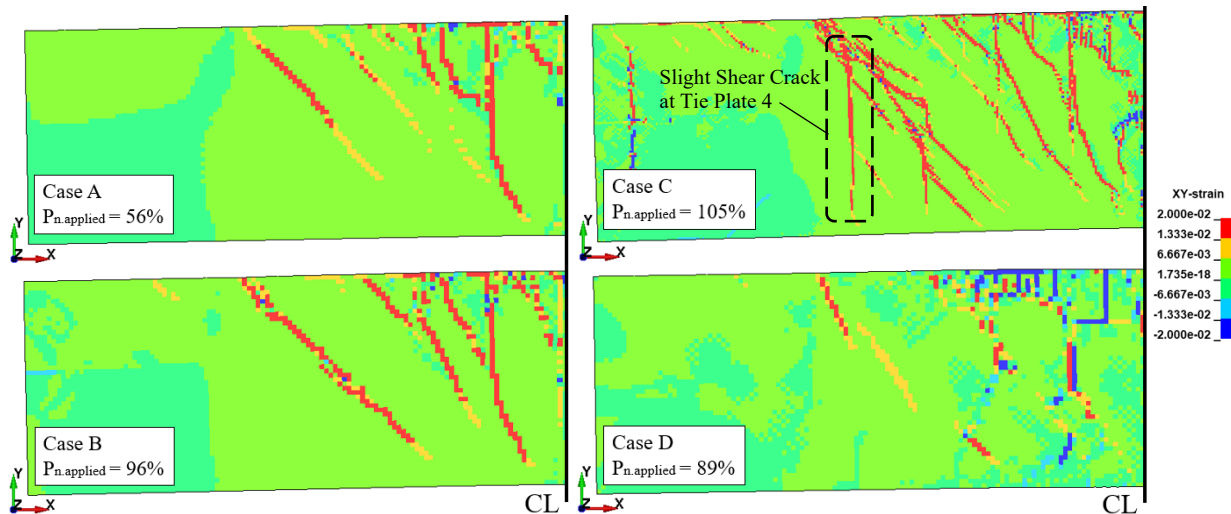


Figure 9. Concrete infill shear strain just prior to failure; ‘Tied’ model realizations. Legend = +/-2%. Displacement scale = 1.

CONCLUSIONS

A parametric study of an SC wall section subject to out-of-plane dynamic loading has been performed. The study assessed two tie plate aspect ratios, two types of loading, and a range of contact definitions. The model geometry and section properties were selected to promote a shear failure, and thus demonstrate the mechanics of the problem. The results indicate that the load carrying capacity of an SC wall section is dependent on both the aspect ratio of the tie plates and the assumed friction between the steel plates and concrete infill. For a typical concrete-to-steel friction value (e.g., $\mu = 0.50$) the reduction in load carrying capacity is ~8% when tie plates with larger aspect ratios are employed. The results also indicate that modeling the steel plates as being tied to the concrete (a common modeling practice) may unconservatively increase the apparent shear capacity of the system. Based on these results, future studies are proposed to investigate (a) the tie plate-to-faceplate connection detail and (b) the SC walls behavior with rotational end restraints. If available, more realistic SC wall configurations, such as those intended for nuclear facilities, should be used in future studies.

PROPOSED FUTURE WORK

Based on the findings of this initial study, future efforts are suggested:

- The results presented herein indicate that the tie plate-to-faceplate connection may experience significant demand and may be a source of premature failure if not properly detailed. Actual connection details (i.e., those utilized by nuclear facilities) likely have reinforcing plates at this connection to reinforce the load path, but this connection may not have been explicitly assessed for out-of-plane loading. Additional assessments of a more representative tie plate-to-faceplate connection is recommended.
- The analysis presented above was for a simply supported SC wall section. Although useful to demonstrate the systems behavior, the configuration is unrealistic for a nuclear facility. Actual configurations will have rotational end restraints (e.g., support provided by orthogonal SC walls) which will develop flexural end moments. Additional assessments of a more realistic wall configuration (i.e., the inclusion of fixed end supports) is suggested to determine the SC wall sections sensitivity to friction when a large compression block (stemming from the end moment) is introduced. If possible, the assessment should include the corner joint with the supporting (orthogonal) SC wall so the complex stress state in the joint can be better understood.

NOMENCLATURE

Case	A unique combination of structural configuration (e.g., faceplate thickness) and load type (e.g. ‘Airplane’ loading). There are 4 total cases.
Model Realization	A unique combination of case (4 total) and contact condition (6 total). There are 24 total model realizations.
Realization	A unique combination of case (4 total), contact condition (6 total), and load curve (125 total). In total, 329 realizations were assessed as part of this study.

REFERENCES

- American Institute of Steel Construction. (2017). *Steel Design Guide 32: Design of Modular Steel-Plate Composite Walls for Safety-Related Nuclear Facilities*. Chicago, Illinois, USA.
- Magallanes, J. M., Wu, Y., Lan, S. and Crawford, J. (2016). “Parameters Influencing Finite Element Results for Concrete Structures,” *SP-306: Analytical and Finite Element Concrete Material Models*, ACI, Farmington Hills, Michigan, 1.1-1.22.
- Nuclear Energy Institute. (2011). *NEI 07-13: Methodology for Performing Aircraft Impact Assessments for New Plant Designs, Rev 8P*. Washington, DC, USA.